# Dynamics in the Water Towers of the Pamir and Downstream Consequences

**Roy Sidle** ( roy.sidle@ucentralasia.org )
University of Central Asia
**Arnaud Caiserman**
University of Central Asia, Mountain Societies Research Institute
**Zulfiqor Khojazoda**
University of Central Asia, Mountain Societies Research Institute
**Álvaro Salazar**
University of Central Asia, Mountain Societies Research Institute

**Article**

**Keywords:**

**Posted Date:** June 17th, 2022

**DOI:** https://doi.org/10.21203/rs.3.rs-1752606/v1



**Additional Declarations:** There is **NO** Competing Interest.

# Abstract

Changes in water delivery from the Pamir Water Towers to streams affect poor regions of Central Asia. We used a 20-yr remotely sensed climate record to assess water source dynamics in the sparsely monitored region. Varying spatial and temporal patterns of rain and snowfall occurred throughout the region. Temperatures increased across the east-central Panj and eastern Vakhsh basins. Warmer temperatures in central Panj and Wakhan corridor coupled with minor declines in snow water will induce water stress during dry years. In contrast, stable temperatures at lower elevations together with increasing precipitation, especially in spring, will benefit agriculture and community water supplies. Seasonal temperature increases, particularly in December, occurred in glaciated areas; however, December temperatures were <-20°C. In the Fedchenko and lower Panj glacier sectors, increasing spring snowfall offsets temperature increases causing little glacier mass change. The Wakhan corridor is at highest risk of glacier mass loss due to declining snow in early spring and increasing temperature in late winter and early spring. Interannual snowfall variability poses the largest uncertainty for water supplies. Permafrost thaw may contribute a small, but timely, source of runoff. Because of high interannual and spatial variability of precipitation, regional climate change scenarios cannot inform adaptation measures for mountain communities, thus, more granular-scale data are needed.


# Introduction

The high elevation Pamir supply most of the water to the Vakhsh and Panj Rivers, which are the major tributaries to the Amu Darya, the largest river in Central Asia. In stark contrast to the great river systems that originate in the Himalayas and Tibetan Plateau that subsequently discharge to the sea, tributaries of the Amu Darya flow downstream through the Pamir leading to arid flatlands in Turkmenistan, along the Turkmenistan-Uzbekistan border, finally discharging into the Aral Sea. The Pamir Water Towers deliver variable seasonal flows to these rivers via snow and glacier melt, rainfall, and permafrost thaw, all of which emanate from the mountainous terrain. This water provides critical livelihood support to poor mountain communities in Tajikistan and Afghanistan, as well as downstream users where climate change and climate variability together with anthropogenic activities affect irrigated agriculture, hydropower, and local water supplies[1–3].

As with most high mountain regions, climate-driven variables that affect the timing and extent of water delivery are unique due to topographic influences, dominance of snow and ice cover, and effects and feedbacks of climate change and variability[4–6]. Based on various anthropogenic stresses on water supplies, population trajectories, and economic development, together with projected climate change effects on precipitation and glacial melt, the Amu Darya basin is ranked at the highest risk for future water availability throughout Asian river basins[7]. Nevertheless, both the environmental and societal consequences of a changing and variable climate in the Pamir related to snow accumulation and melt; glacial melt; permafrost thaw; and rainfall have not been assessed in a holistic manner, particularly how such spatial and temporal changes will impact poor mountain societies and downstream water users.

The Pamir lies in a continental collision zone formed by the convergence of the Tien Shan to the north, Hindu Kush to the southwest, Himalaya to the southeast, and Karakoram and Kunlun Shen to the east. Most of the Pamir are in Tajikistan with small portions in northeast Afghanistan and northwest China. The western Pamir receive higher precipitation, particularly in winter, than the eastern Pamir due to mid-latitude westerlies, reflected in the higher altitude glacier snowlines east of Ismoil Somoni massif (7495 m)[8]. Glaciers occupy a substantial percentage of various catchments of the Pamir ranging from 5% in Kyzylsu River basin (eastern Pamir) to 29% in Muksu basin (central Pamir) where the 77 km long Fedchenko Glacier exists in an area with the highest recorded annual precipitation (1180 mm)[9]. An arid high plateau (> 4000 m a.s.l.) extends across the eastern Pamir with scattered glaciers along high ridges.

Recognizing that precipitation is the main driver of regional water supplies, it is noteworthy that both the spatial coverage and number of meteorological stations in the Pamir are sparse and typically confined to lower elevations. Furthermore, precipitation records are rather short, and the few longer records have considerable data gaps during the 1990's coinciding with the breakup of the former Soviet Union. Throughout much of Central Asia, a declining trend in the snowfall fraction of total precipitation is predicted[10]; however, interannual snow properties appear highly variable[11]. The only systematic study in this region to address runoff contributions used MODIS-derived remote sensing products to estimate melt contributions of snow (65%), glaciers (8%), and snow on ice (4%) to runoff above 2000 m a.s.l. within the entire Amu Darya basin; rainfall contributions (23%) were estimated from monthly spatially interpolated precipitation data (APHRODITE)[12]. While these estimates provide a broad depiction of various sources, contributions to the discharge regime of tributaries differ drastically depending on the presence or absence of glaciers, basin elevation, orography, temperature, geographic location, and the granularity of precipitation data. Semi-distributed hydrological models employing APHRODITE precipitation with assumptions on flow contributions have yielded higher estimates of glacier runoff[13,14]. Some studies in the Pamir have reported glacier area shrinkage[15–18], while others suggest that although glaciated areas might be decreasing, in many cases little ice mass change has occurred, as noted in the Pamir-Karakoram anomaly[19–25]. While permafrost has been overlooked as a potential contributor to runoff, its wide distribution across the high Pamir and response to climate change may inform whether permafrost thaw contributions to seasonal discharge warrant inclusion in models. Remotely sensed precipitation and temperature data in this cryosphere-dominated landscape can help quantify how local runoff sources affect stream discharge and these granular data provide more robust predictions for down-river users, such as hydropower projects and irrigated agriculture.

To address the underlying issues of distribution of Pamir water sources and their effect on local and downstream water supplies, we examine the nexus between climate and water supply dynamics considering both environmental and social consequences. To emphasize this nexus, we show trends of solid and liquid precipitation and temperature during the past 20 year in the Pamir. We illustrate these dynamics and potential impacts through relevant examples with due consideration to spatial variability and local effects that will impact poor mountain communities.

# Results

**Dynamic Rain and Snowfall Patterns.** Average annual precipitation derived from remote sensing ranges from 325 mm at elevations > 4500 m a.s.l. to 622 mm at elevations < 2225 m a.s.l. (Table 1). Temperature estimates derived from MODIS Land Surface Temperature & Emissivity (LST&E) (MOD11A1) were used to separate liquid from solid precipitation. Snow accounts for 76% of total precipitation at high elevations compared to 42% at elevations < 2225 m. During the 20-yr period from 2001 to 2020, there was a slight but insignificant overall increase in total precipitation in the Pamir region.

Table 1
Average annual precipitation components and temperatures throughout the Pamir in different elevation bands for the period from 2001 to 2020.

| | < 2225 m a.s.l. | 2225–4500 m a.s.l. | > 4500 m a.s.l. |
|---|---|---|---|
| Total average annual precipitation (mm) | 622 | 475 | 325.5 |
| Average annual rainfall (mm) | 360 | 178 | 78.5 |
| Range in annual rainfall (mm) | 218–457 | 113–239 | 35.7–118 |
| Average annual snowfall (mm) | 262 | 297 | 247 |
| Range in annual snowfall (mm) | 144–356 | 194–355 | 173–304 |
| % precipitation as snow | 42% | 63% | 76% |
| Average annual temperature (°C) | 15.9 | − 0.9 | − 9.6 |
| Range in annual temperature (°C) | 14.4 to 17.5 | − 2.5 to 0.7 | -11.5 to − 8.0 |

Focusing on snow water at a scale of 10 x 10 km, some significant patterns emerge in the different elevation zones during this 20-yr period (Fig. 1a). For the combined areas above 4500 m, annual snow accumulation did not significantly change with time, but increases occurred during spring to mid-summer (0.29 mm $y^{-1}$) and decreases in snowfall occurred in early fall to early winter (largest decrease in December; − 0.88 mm $y^{-1}$). Mid-elevations (2225–4500 m) experienced overall weak (insignificant) positive trends in snowfall with a negative trend occurring in late summer to early fall. At lower elevations, a positive trend in annual snowfall was observed, particularly evident in late spring (1.3 mm $y^{-1}$; Fig. 1b). Snowfall increases were primarily concentrated in broad valleys of the Vakhsh River upstream of the Nurek reservoir. Many mid to high elevation areas in Vakhsh basin also had significant snowfall increases (Fig. 1a). In contrast, some mid-elevation areas of the central Panj basin experienced small increases in snow while other areas had minor decreases.

Spatial and temporal patterns of annual rainfall differed at various elevations (Fig. 1c). Above 2225 m, no overall temporal trends in rainfall were detected, although total precipitation increased in spring. At mid-elevations (2225–4500 m), snow water inputs declined in late summer; however, annual trends were slightly positive, but insignificant. Snow water inputs increased in early summer above 4500 m but

decreased in early winter; no annual trends were observed. Isolated areas of rainfall decline occurred in higher parts of eastern Vakhsh basin, whereas throughout most of the mid to high elevation Panj basin, many areas experienced increased rainfall (Fig. 1c). The southern-most portion of the Panji basin in Afghanistan had isolated areas of rainfall decline. The largest increases in annual rainfall occurred throughout western portions of the Vakhsh and Panj basins (elevations < 2225 m). Overall, annual rainfall below 2225 m increased significantly during the 20-yr period at a rate of ≈ 0.5 mm $y^{-1}$ (Fig. 1d), with the greatest increases in spring and early fall.

**Snow Persistence and Snowline Elevation Trends.** Trends in snow persistence (SP; fraction of a year that snow is present on the ground) can help inform climate change. Mean SP in the Vakhsh and Panj basins varied between 0.45 ± 0.28 and 0.54 ± 0.3 from 2000 to 2020 (Fig. 2a). Interannual SP variability was rather high and no significant temporal trends occurred. The lowest SP values, 0.45 and 0.47, occurred during 2007 and 2008, respectively (Fig. 2b) and were mainly at mid and high elevations (i.e., > 2225 m; Fig. 2a). SP values in the mid and high elevations during the 20-yr period averaged 0.54 ± 0.2 and 0.79 ± 0.15, respectively. In contrast, low elevations (< 2225 m) had a mean SP value of 0.13 ± 0.13 with high interannual variability. The highest SP values were observed during 2009 below 2225 m with values ranging from 0.60 ± 0.19 at mid-elevation to 0.85 ± 0.12 at high elevations.

Another insight into climate change in the cryosphere can be derived from the evolution of long-term snowline elevations. Snow precipitation and coverage varied widely from one winter to another; however, snow elevations may evolve over decades due to climate change. Results of remote sensing analysis (see Methods) throughout the entire Vakhsh and Panj basins showed no significant trends of monthly snowline elevation. However, when examining only the high elevation range (4500–7495 m), small, but significant, increases in snowline elevations of 2.57 m $yr^{-1}$ (p-value: 0.03) and 1.23 m $yr^{-1}$ (p-value: 0.04) appeared in November and February, respectively, since 2001 (Fig. 2c). This means that the snow coverage tended to decrease since 2000. This increasing elevation of snowline in early winter is consistent with the significant decreasing trend of snowfall in December (− 0.88 mm $y^{-1}$) since 2000. Early winter is receiving less snow than in the past leading to a higher snowline after that time of the year.

**Temperature trends.** Temperature trends are important to understand how observed patterns of rain and snow relate to runoff. There are major temperature gradients across the Vakhsh and Panj basins with the highest temperatures in the western region grading sharply to lower temperatures at high elevations to the east (Table 1). Slightly increasing air temperatures during the 20-yr period occurred in parts of the high elevation glaciated areas in the Vakhsh basin (Fig. 3). Climate warming ‘hot spots’ are seen in the mid-high to high elevation central and southeast portions of the Pamir (Fig. 3). However, it is notable that these areas have alpine climates with low precipitation, thus any effects of climate warming on runoff produced from these areas may be minimal and considerably delayed. Interestingly, below 2225 m, temperature has been relatively stable during the 20-yr period, including terrain proximate to the Vakhsh River and its major tributaries (Fig. 3). These areas with little temperature increase correspond to some of the most productive agricultural lands in Tajikistan.

**Other Dynamic Water Sources: Glacier Melt and Permafrost Thaw.** Based on the World Glacial Inventory (https://nsidc.org/data/g011w230), about 5.5% of the total area of Tajikistan is covered by glaciers making it one of the most glaciated nations worldwide. The 'supply index' partly associated with glacier volume and water yield in the Amu Darya basin is higher than most major river basins[26]. Because more than half of the land area of Tajikistan is above 3000 m, 44% of the country has been identified as potential permafrost area[27]. Most of this permafrost is concentrated in the high-elevation Badakhshan region of the southern and eastern Pamir in Tajikistan and northern Afghanistan.

Approximately 13,000 glaciers reside in the Pamir (ice volume of 1300 $km^3$)[28], and about 8% of total discharge in the Amu Darya emanates from these[12]. Investigations of glacier area and mass change in the Pamir conducted in the past decade have shown different results based on geography, methods used, and time periods. To normalize these diverse findings, we employed a systematic literature review that revealed glacial mass loss is not necessarily directly related to glacier area. Elevational changes in Pamir glaciers estimated by various methods are typically less than or within the range of error estimates (Table 2). Studies in the adjacent Western Kunlun indicate minor, but significant, glacial elevation increases[21,23]. Other studies in the circum-Pamir show small gains of glacier mass during the first decade of this century followed by small losses; however, these values are mostly within error estimates[24, 29]. Studies at specific sites revealed opposite patterns or very little change in glacial mass during this century[20,22,25]. A recent study in the central Pamir concluded that glacier mass budgets were approximately balanced or had slight mass deficits from mid-1970's to mid-2010's[30]. Our summary of studies throughout the wider Pamir region confirms these findings (Table 2).

Table 2
Recent studies using various remote sensing techniques estimating glacial mass change (using elevation change as an indicator) within and proximate to the Pamir.

| Specific Location | Glacier area | Elevation (m a.s.l.) | Glacial elevation change per year | Methodology | Source |
|---|---|---|---|---|---|
| Eastern Pamir, W. China<br><br>38-39°N, 73-75°E | 2362.5 $km^2$ | 3000 to > 7600 | -0.06 ± 0.16 m (2000–2009)<br><br>0.06 ± 0.04 m (2000–2016) | Geodetic using: SRTM, NASA HMA & ALOS-PRISM DEMs | Lv et al. 2020 |
| Eastern Pamir, NW China<br><br>38-39°N, 74°40’ – 75°40’E | 1018 to 999 $km^2$ | 3000 to 7719 | -0.15 ± 0.12 m (≈ 1971 – ≈2013) | ASTER, Cartosat-1, Landsat, SRTM DEMs, topographic maps & glacier inventories | Zhang et al. 2016 |
| Eastern Pamir, Xinjiang, China 38°17’N; 75°07’E | 274 $km^2$ | up to 7546 | -0.01 ± 0.30 m (1973–2013) | Geodetic using: Hexagon KH-9, ALOS-PRISM, Pléiades, Landsat & SRTM DEM | Holzer et al. 2015 |
| Central Pamir | 2120 $km^2$ | – | -0.03 ± 0.24 m (1975–1999) | Randolph Glacier Inventory, KH-9 stereo images, SRTM DEM | Zhou et al. 2019 |
| Western Pamir | 3178 $km^2$ | 2800 to 7090 | 0.14 ± 0.13 m (1999–2011) | SRTM DEMs & SPOT5 stereo images | Gardelle et al. 2013 |
| Pamir | 1000 ± 300 elev. Samples | – | -0.46 ± 0.28 m (2003–2008) | ICESat altimetry data, SRTM DEM | Wang et al. 2017 |
| Pamir | 4441 $km^2$ | 3600 to 5750 | -0.05 ± 0.08 m (2000–2016) | ASTER DEMs | Brun et al. 2017 |
| Pamir, Panj River basin | > 2000 $km^2$ | 800 to > 7000 | -0.52 m (2002–2013) also considers snow | Empirical, lumped hydrological model estimates (J2000g) | Pohl et al. 2017 |
| Pamir | 6500 $km^2$ | – | -0.48 ± 0.14 m (2003–2008) | ICESat altimetry data | Kääb et al. 2015 |
| Pamir Alay | 809 $km^2$ | 3300 to 4600 | -0.04 ± 0.07 m (2000–2016) | ASTER DEMs | Brun et al. 2017 |

| Specific Location | Glacier area | Elevation (m a.s.l.) | Glacial elevation change per year | Methodology | Source |
|---|---|---|---|---|---|
| West Kunlun, Xinjiang, China<br><br>35-36°N, 82-83°E | 1687 to 1695 $km^2$ | 5000 to 7000 | 0.26 ± 0.07 m (2000–2016) | ASTER DEMs | Brun et al. 2017 |
| West Kunlun, NW China | 12,500 $km^2$ | – | 0.05 ± 0.07 m (2003–2008) | ICESat altimetry data | Kääb et al. 2015 |

Given the scattered distribution of glacier studies in the Pamir, we examined precipitation and temperature parameters within six glaciated regions: Fann mountains, Pamir-Alay range, Fedchenko region, central Pamir, lower Panj basin, and Wakhan corridor (Fig. 4). Remote sensing analysis of solid precipitation and temperature during the last 20 year revealed some significant short-term trends for these climate parameters in most sub-regions (Fig. 4). All sub-regions experienced a significant increase in December temperature, while only the Fann, Fedchenko, and Pamir-Alay sectors had significant increases in annual temperature during the 20-yr period. Although warming dominated in December, temperatures were much lower than − 20°C in all regions. Thus, in the foreseeable future, these increases should not affect glacier melting. Furthermore, from early winter to early spring, a few short-term (4-week) temperature increases were observed in the lower Panj, central Pamir, Pamir-Alay, and Wakhan (Fig. 4). For other periods, temperature trends were highly variable with time. Snowfall exhibited no significant annual trends in all glaciated areas. Significant short-term decreases in snowfall occurred in the central Pamir (December), Pamir-Alay (late summer), and Wakhan corridor (March). In contrast, Fedchenko and lower Panj received increasing snowfall from 23 April to 20 May over the 20-yr period (Fig. 4). These late spring increases in snowfall will likely offset the winter temperature increases and help maintain glacier ice mass.

While glacial melt is usually assumed to contribute directly to streamflow[3,14,31–33], runoff generated from melting glaciers in high elevation plateaus may be partly or even completely disconnected from major streams and rivers[11,34]. Glacial melt can recharge shallow or deep groundwater reservoirs, which eventually support baseflow in streams[32,35], but in high glaciated plateaus such contributions may be small. These complex hydrogeomorphic effects are not captured in any of the hydrological models currently applied in this region. To elucidate the connectivity of glacial melt to streams, we overlaid maps of glaciers in this area on a digital elevation model (Alos Palsar 12.5 m) containing stream networks to provide better estimates of melt contributions (Fig. 5). Results showed that about 75% of Pamir glaciers were closely connected to first-order or larger channels in the Vakhsh-Panj basin. This analysis somewhat overestimates connectivity because some first-order streams are not connected to major river systems. Nevertheless, this points to invalid assumptions often made that all glacial melt is delivered to rivers and that all changes in melt will affect river discharge[14,34].

Wide areas of permafrost exist in the Pamir-Alay (≈ 50,000 $km^2$) and the Tien Shan (≈ 5500 $km^2$), with continuous permafrost beginning at elevations of 4000 m and 3500 m, respectively[36]. Discontinuous and sporadic permafrost typically begins at elevations of about 300 to 400 m and 600 to 800 m lower than continuous permafrost, respectively. Based on the TTOP model[37], we estimate that 23,951 $km^2$ of continuous permafrost terrain exists in the Panj and Vakhsh basins (14% of the combined Panj-Vakhsh basin), with the majority located in eastern Tajikistan and the Wakhan corridor of Afghanistan at elevations > 3577 m (Fig. 6). Permafrost in most areas underlies the 'active layer', which is about < 1 to > 2 m thick and seasonally thaws and refreezes in response to thermal changes[37].

Given that no studies have quantified streamflow contributions from summer thaw of the active layer, we estimated this contribution for current conditions in the outlined areas (i.e., Fig. 6) of the Pamir. Active layer thickness (ALT) is inversely related to elevation with current estimates ranging from 1 m (> 4700 m) to 3.5 m (< 4400 m)[38]. Streamflow contributions from permafrost thaw during July through August were calculated as subsurface flux from streambanks by adapting research findings from field studies in a similar environment[39] and scaling them to different stream orders in the Vakhsh and Panj basins (see Methods). Stream and river segments were segregated into small (first- and second-order), medium-size (third-order), and large (fourth-order and above) reaches comprising channel lengths of 18,920.7, 2347.0, and 578.3 km, respectively, within the combined basins. Estimated total permafrost contribution to streamflow during the 2-month melt season was 638 x $10^6$ $m^3$, about 1.5% of the average annual river discharge for the combined Vakhsh-Panj basins. More than two-thirds of this contribution emerged in first and second-order streams, which were more numerous and where the entire streambank height (0.5 m) was assumed to consist of an active layer. Permafrost contributions from third- and higher-order channels were 0.33% and 0.16%, respectively, of average annual basin flows.

# Discussion And Implications

Some interesting and spatially inconsistent trends in liquid and solid precipitation emerged across the Vakhsh and Panj River basins during the past 20 year based on remote sensing analyses. The most important change is an increase in rainfall below 4500 m a.s.l., with the largest increases occurring in spring in the western portions of these basins (Fig. 1c). Coupled with a lack of any significant warming trends at lower elevations, these increases bode well for irrigated agriculture and community water supplies in western Tajikistan. Similarly, slight increases in snow in the northern part of the basin may benefit farmers in the near term (Fig. 1a). In contrast, temperatures in the north and central portions of the basin are increasing. Some locations of the central Pamir appear to be shifting from snow to rain, approximately offsetting each other, but likely producing more runoff in late spring to early summer and less in mid to late summer. Future water supplies in this dry region may be vulnerable, although given the very low annual temperatures at high elevations (Table 1), it will take many years for changes in runoff to occur. Similar future changes are likely in the far eastern portion of the Panj basin, but again this alpine area receives very little precipitation and is extremely cold. In contrast to the Panj basin, snowfall is increasing in many high elevation areas of the Vakhsh basin and rainfall is declining slightly in scattered

areas. Across the entire study area, both snow persistence and snowline elevation were variable from year to year with no significant long-term trends; only above 4500 m a small, but significant, increase in snowline elevation occurred indicating a possible effect of climate warming (Fig. 2c).

Temperature regime is frequently noted as a major influence in glacier mass change[17,40], but it is certainly not the only factor. Precipitation (primarily snow amount and distribution), regional climate circulation patterns, surface albedo, topography, elevation, glacier hypsometry, humidity, deposition of black carbon and dust, variations in glacier velocity, and overall glacier physics all affect changes in glacial mass[8,16,24,41–43]. Glacier growth in the region is mainly attributed to increases in snowfall[44,45]. Several studies that have shown short-term negative mass balances noted that precipitation inputs (mostly snow) are more important determinants than temperature changes[29,44]. Surging glaciers, common in the Pamir, do not appear to significantly affect glacier mass balance over decades[24,46]; however, the displacement of ice to lower elevations could eventually enhance melting.

In most glaciated catchments within the upper Panj basin, higher temperatures are expected to increase stream discharge; however, as melting glaciers reach their tipping point such increases will cease and once the glaciers disconnect or completely melt, discharge will abruptly decline. This pattern is being observed in certain glaciated headwater catchments in the Kunduz River (Afghanistan), which feeds the Panj River; however, droughts since the 1960's coupled with land cover changes have caused strong decreases in down-river discharge[33]. Recent investigations we reviewed indicate uncertainties and complexities inherent in remotely quantified changes in glacial mass, which will affect water delivery to streams (Table 2)[17,22,23,47]. Some high-elevation glaciated regions in the upper Vakhsh basin (Fedchenko and Fann) are receiving increased snowfall that will likely reduce the impact of temperature increases in these regions, thus maintaining the minimal reported mass change in glaciers[20,21,23,30]. Based on precipitation and temperature trends, it appears that glacial mass changes will be minimal in most sub-regions, with the Wakhan corridor being an exception due to declining precipitation and early spring warming. Thus, in Wakhan, runoff derived from glacier and permafrost melt could emanate earlier and increase as warming continues. For example, in a climate change 'hot spot' in the Panj basin, south and east of Murghab and just north of the Wakhan Corridor (3700 to > 5000 m a.s.l.), small mountain glaciers appear to be disappearing, with some reaching tipping points. Minor increases in permafrost contributions to runoff can be expected in high elevation streams due to warming and these may be sustained for a long time. Some areas of the central Pamir experienced increases in rain and decreases in snow water equivalent; thus, where such changes occur in glaciated terrain, melt will increase and occur earlier until glacier mass is exhausted and tipping points are reached. Hence, this dry central Pamir area is at high risk for long-term future water supplies, although given the very low annual temperatures above 4500 m (Table 1), it may take many years for such changes to occur.

A few studies have noted the major challenge of quantifying the connectivity of various high mountain runoff sources to streams and rivers[15,27]. Additionally, understanding how much runoff from the Pamir recharges groundwater in alluvial valleys and plains is poorly understood[13]. The hydrological connectivity

of various water sources to streams, particularly glacier melt in remote regions, can inform how climate change may differentially impact such sources throughout drainage basins. Spatial and temporal connectivity of snow and permafrost melt are also important determinants of water supplies to streams, requiring detailed assessments to clarify these issues[34].

Given our knowledge of orographic effects on precipitation, it is not surprising that a range of climate patterns and trajectories are evident in the Vakhsh and Panj basins. These changes pose challenges for predicting runoff from high elevation cold regions due to the altered patterns of the timing of snow, glacier, and permafrost accumulation and melt, including temporal changes, interannual variability, and hydrological connectivity of sources[34]. Various water sources will respond differently in a changing climate, generating complex runoff scenarios and socioeconomic consequences downstream. Given that glacier melt coincides with the growing season, changes in the amount and timing of melt may have significant impacts on agriculture[3]. Moving forward, modelling efforts need to consider these climate and runoff generation dynamics to ensure more spatially explicit outcomes[34]. This applies not only to the Pamir, but also other high mountain regions of Asia where such granular information is essential for supporting livelihoods and food security in poor communities, particularly for developing climate-smart agricultural, selecting appropriate seed sources and crops, assessing drought tolerance, and ensuring sustainable potable water supplies. In the Amu Darya basin, down-river hydropower plants and consumptive users of water must understand how flow regimes may change to ensure optimal management. Our study provides a segue into this complex biophysical and socioeconomic arena and clearly shows that climate analyses at detailed scales are needed to address water user concerns.

# Methods

**Total Precipitation Trend Analysis using IMERG V06**. Spatial and temporal precipitation trends across the Vakhsh and Panj basins were calculated using daily GPM IMERG V06 Final Run from 2001 to 2020. Of the three options of IMERG data (Early, Late and Final Runs), we used the research grade Final Run data with a resolution of 0.1 x 0.1 degrees or approximately 10 x 10 km. Average precipitation across the entire Vakhsh and Panj basins was calculated for annual, seasonal, and 4-week periods. The study area was then divided into three elevation bands (317–2225 m, 2225–4500 m, and 4500–7543 m) and 20-yr average precipitation trends in each elevation band were analyzed (threshold p-value = 0.05). Spatial trends were assessed on a pixel basis with the trend for each pixel calculated as:

$$m = \frac{n(\sum xy) - (\sum x)(\sum y)}{n(\sum x^2) - (\sum x)^2} \qquad [1]$$

where, $m$ is the slope of the trend, $n$ is the number of years (in our case 20, from 2001 to 2020), $x$ is the specific year, and $y$ is the average precipitation over an area or a value for each grid in the same year as $x$. Positive slopes represent increasing trends and negative slopes represent decreasing trends. The p-values

for significant slopes are assessed as < 0.05 and only the pixels with significant trends were plotted on the maps in color.

**Land Surface Temperature Trend Analysis and Snow and Rainfall Separation and Analysis using MODIS.** MODIS Land Surface Temperature & Emissivity (LST&E) (MOD11A1) Day and Night was used to separate liquid and solid precipitation. MOD11A1 contained gaps due to clouds. Averages of Day and Night and seven calendar days were calculated to decrease the gaps. The remaining gaps were filled in a GIS program using the following code: *(Con(IsNull("raster"), FocalStatistics("raster", NbrRectangle(5,5, "CELL"), "MEAN"), "raster"))*. The IMERG precipitation data overlaid with MOD11A1 surface temperatures < 0°C were considered solid precipitation and precipitation values with MOD11A1 surface temperatures ≥ 0°C represent liquid precipitation. The spatial resolution of IMERG data and MOD11A1 are different. Since the spatial resolution of IMERG is 10 x 10 km compared to 1 km x 1 km for MOD11A1, MODIS layers were resampled to match the spatial resolution of IMERG. In doing so, average temperature of the resampled area was calculated. Therefore, the resampled 10 x 10 km MOD11A1 layer contains the average of the 1 x 1 km pixels within it. Liquid and solid precipitation were analyzed separately across the study area based on elevation bands and spatial trends were calculated similar to those for IMERG total precipitation.

**Snow Persistence and Snowline Trend Analysis using MODIS.** Snow persistence (SP) is the fraction of a year during which snow is present on the ground (dimensionless). We calculated SP for the study area using Moderate Resolution Imaging Spectroradiometer (MODIS) MOD10A Collection 6 (C6) snow product at 500 m spatial resolution daily snow cover extent between years 2000 and 2020. C6 has been significantly improved compared to Collection 5 and data have been substantially increased[48].

Using the visible and infrared bands of MODIS, the snow detection algorithm applies the normalized differential snow index (NDSI). NDSI gives the magnitude of the difference between very high reflectance in visible bands and the very low reflectance in the shortwave infrared of land areas covered by snow. Each daily observation of MOD10A1 represents the best sensor view of the surface in the cell based on solar elevation, distance from nadir, and cell coverage[48]. Different pixel values represent various surface features, e.g., 239 for ocean; 250 for clouds, and 0-100 for NDSI snow cover.

We downloaded MOD10A1 from the Application for Extracting and Exploring Analysis Ready Samples (AppEEARS) website as netCDF format with geographic projection and datum WGS84. Snow data (pixels with values 0-100) were then extracted using Python programming language, selecting the best pixels based on the quality assessment layers (QA). For each date, we reclassified the pixels with snow as 1, leaving all other values as 0. The sum of all images for each year were calculated giving the number of images with snow presence for each year. Yearly SP was obtained after dividing the number of times a pixel was snow covered by the total number of MOD10A1 images for that specific year. SP less than 7% was discarded to account for classification errors.

Snowline evolution was assessed using MOD10A2.006 (https://nsidc.org/data/MOD10A2/versions/6), a remote sensing product that provides worldwide snow coverage on an 8-day basis since 2000 (500 m

resolution). Images were collected and compiled in monthly intervals for the last 21 year for the entire area with a specific focus on high elevations (4500 to 7495 m). Indeed, higher elevations should be analyzed separately since the snow cover remains year-round. Mean snowline elevations each month were calculated, and a Mann-Kendall test was performed using a p-value 0.05 threshold to test for a significant trend.

**Permafrost Contribution using SRTM-30.** To estimate current inputs of permafrost thaw to streamflow within the Panj and Vakhsh basin, we first assessed permafrost distribution in the Pamir using the TTOP model, which provides permafrost zonation at a 1 $km^2$ scale based on remotely sensed land surface temperature, the ERA Interim climate reanalysis model, and landcover data[37]. A mask was then created in the DEM to capture streams within permafrost areas (SRTM-30). These were then identified by stream-order; first- and second-order streams are assigned bank heights of 0.5 m, third-order streams are assigned bank heights of 1.0 m, and higher-order streams are assigned bank heights of 3 m based on field investigations and aerial images. Stream lengths for all stream orders were inventoried in GIS. Active layer thickness was estimated as 1.5 m for areas proximate to first- through third-order streams and 3 m for larger streams located at lower elevations[49]. A melt season of 60 days in July and August was assumed when air temperatures were > 0°C.

Saturated subsurface flux emanating from streambanks due to permafrost thaw was adapted from results of a study of snowmelt discharge from a soil pit excavated in similar glaciated terrain[39]. We used lower cumulative flux values for the 60-day period due to the drier nature of our terrain: 300 $m^3\ m^{-2}$ for the 0-0.5 m depth; 150 $m^3\ m^{-2}$ for the 0.5-1.0 m depth; and 30 $m^3\ m^{-2}$ for the 1–3 m depth. These decreasing values of subsurface flux with depth are based on the common assumption that saturated hydraulic conductivity ($K_s$) declines as an exponential function of soil depth[50] verified by data from permafrost terrain[51]. Finally, we specified vertical 'leakage' losses (flow that does not emerge from the streambank) for specific soil depths as follows: 90% at the base of the 0-0.5 m depth (due to higher $K_s$ in this soil); 70% below the 0.5-1.0 m depth (less leakage due to $K_s$ discontinuity below this layer); and an additional 85% below the 1–3 m depth. Such assumed leakage losses are in the range or slightly higher than values reported for forest soils underlain by bedrock[52]. Thus, we believe our estimated flux to channels was conservative.

For each specified soil depth at the streambank interface (i.e., 0-0.5 m; 0.5-1.0 m; and 1–3 m), the volume of flow during the 60-day melt season ($V_{60}$) was calculated as:

$$V_{60} = 2L \bullet D \bullet F_s \bullet p_L \quad [2]$$

where, $V_{60}$ is the total volume of subsurface flow from each soil layer for the 60-day melt period ($m^3$); 2L is the length of the stream channel segment x 2 banks (m); D is the vertical streambank height: 0.5 m for first- and second-order streams, 1.0 m for third-order streams, and 3 m for higher order streams; $F_s$ is the cumulative flux rates ($m^3\ m^{-2}$) representing flow per $m^2$ of streambank area during the entire 60-day melt

season; and $p_L$ is leakage below the specified depth that does not flow from the streambank. These volumetric calculations are then summed for all stream segments in each of the three stream-order categories.

# Declarations


### Acknowledgements

A portion of the snow-related research included in this paper was supported by the European Union and executed through a grant focused on “Addressing Climate Change in Afghanistan (E3C)” as part of “Improve Participatory Management and Efficiency of Rangelands and Watersheds” implemented jointly by the Aga Khan Foundation, Wildlife Conservation Society, and GTZ in the Panj Amu River Basin of Afghanistan under EU CRIS contract number: ACA/2018/399-677.


### DECLARATION OF INTERESTS

The authors declare no competing interests.

# References


1. White, C.J., Tanton, T.W. & Rycroft, D.W. The impact of climate change on the water resources of the Amu Darya basin in Central Asia. *Water Resour. Manage.* **28**, 5267–5281 (2014).
2. Jalilov, S.-M., Amer, S.A. & Ward, F.A. Managing the water-energy-food nexus: Opportunities in Central Asia. *J. Hydrol.* **557**, 407–425 (2018).
3. Gulakhmadov, A. et al. Simulation of the potential impacts of projected climate change on streamflow in the Vakhsh River Basin in Central Asia under CMIP5 RCP scenarios. *Water* **12**, 1426 (2020).
4. Beniston, M., Diaz, H.F., & Bradley, R.S. Climate change at high elevation sites: an overview. *Climate Change* **36**, 233–251 (1997).
5. Rangwala, I. & Miller, J.R. Climate change in mountains: a review of elevation-dependent warming and its possible causes. *Climate Change* **114**, 527–547 (2012).
6. Thornton, J.M. et al. Toward a definition of essential mountain climate variables. *One Earth* **4**, 805–827 (2021).
7. Immerzeel, W.W. & Bierkens, M.F.P. Asia’s water balance. *Nature Geosci.* **5**: 841–842 (2012).
8. Stübner, K., Bookhagen, B., Merchel, S., Lachner, J. & Gadoev, M. Unraveling the Pleistocene glacial history of the Pamir mountains, Central Asia. *Quarter. Sci. Rev.* **257**, 106857 (2021).
9. Chevallier, P., Pouyaud, B., Mojaïsky, M., Bolgov, M. Olsson, O., Bauer, M., Froebrich, J. River flow regime and snow cover of the Pamir Alay (Central Asia) in a changing climate. *Hydrol. Sci. J.* **59**, 1491–1506 (2014).

10. Li, Z., Chen, Y., Li, Y. & Wang, Y. Declining snowfall fraction in the alpine regions, Central Asia. *Scient. Rep.* **10**, 3476 (2020).
11. Murzakulova, A. & Sidle, R.C. Rethinking the nexus of climate change, development and discourse of danger in Central Asia. *MSRI Brief*, Mountain Societies Res. Inst., Univ. of Central Asia, 4 p. (2020).
12. Armstrong, R.L. et al. Runoff from glacial ice and seasonal snow in High Asia: separating melt water sources in river flow. *Region. Environ. Change* **19**, 1249–1261 (2019).
13. Pohl, E., Gloaguen, R., Andermann, C. & Knoche, M. Glacier melt buffers river runoff in the Pamir Mountains. *Water Resour. Res.* **53**, 2467–2489 (2017).
14. Pohl, E., Knoche, M., Gloaguen, R., Andermann, C. & Krause, P. Sensitivity analysis and implications for surface processes from a hydrological modelling approach in the Gunt Catchment, high Pamir mountains. *Earth Surf. Dynam.* **3**, 333–362 (2015).
15. Hoelzle, M. et al. The status and role of the alpine cryosphere in Central Asia. In: Xenarios, S. et al. (eds.) *The Aral Sea Basin – Water for Sustainable Development in Central Asia*, Ch. 8. pp. 100–121, Routledge, London (2020).
16. Khromova, T.E., Osipova, G.B., Tsvetkov, D.G., Dyurgerov, M.B., Barry, R.G. Changes in glacier extent in the eastern Pamir, Central Asia, determined from historical data and ASTER imagery. *Remote Sens. Environ.* **102**, 24–32 (2006).
17. Haritashya, U.K., Bishop, M.P., Shroder, J.F., Bush, A.B.G. & Bulley, H.N.N. Space-based assessment of glacial fluctuations in the Wakhan Pamir, Afghanistan. *Climatic Change* **94**, 5–18 (2009).
18. Bishop, M.P. et al. Remote sensing of glaciers in Afghanistan and Pakistan. Chapter 23, In: Kargel, J.S. et al. (eds.), *Global Land Ice Measurements from Space*, Springer, Berlin (2014).
19. Zhao, L., Ding, R. & Moore, J.C. Glacier volume and area change by 2050 in high mountain Asia. *Global Planet. Change* **122**, 197–207 (2014).
20. Holzer, N. et al. Four decades of glacier variations at Muztagh Ata (eastern Pamir): a multi-sensor study including Hexagon KH-9 and Pléiades data. *The Cryosphere* **9**, 2071–2088 (2015).
21. Kääb, A., Treichler, D., Nuth, C. & Berthier, E. Brief communication: Contending estimates of 2003–2008 glacier mass balance over the Pamir-Karakoram-Himalaya. *The Cryosphere* **9**, 557–564 (2015).
22. Zhang, Z. et al. Mass change on glaciers in Muztag Ata-Kongur Tagh, eastern Pamir, China from 1971/76 to 2013/14 as derived from remote sensing data. *PLoS ONE* **11**, e0147327 (2016).
23. Brun, F., Berthier, E., Wagnon, P., Kääb, A., & Treichler, D. A spatially resolved estimate of High Mountain Asia glacier mass balances, 2000–2016. *Nature Geosci.* **10**(9), 668–673 (2017).
24. Lv, M. et al. Examining geodetic glacier mass balance in the eastern Pamir transition zone. *J. Glaciol.* **66**(260), 927–937 (2020).
25. Kronenberg, M., Machguth, H., Eichler, A., Schwikowski, M. & Hoelzle, M. Comparison of historical and recent accumulation rates on Abramov Glacier, Pamir Alay. *J. Glaciol.* **67**(262), 253–268 (2021).
26. Immerzeel, W.W. et al. Importance and vulnerability of the world's water towers. *Nature* **577**, 364–369 (2020).

27. Mergili, M., Kopf, C., Müllebner, B. & Schneider, J.F. Changes of the cryosphere and related geohazards in the high-mountain areas of Tajikistan and Austria: a comparison. *Geograf. Ann.: Ser. A, Phys. Geog.* **94**, 79–96 (2012).
28. Aizen, V.B. Pamir glaciers. In: Singh, V.P., Singh, P, and Haritashya, U.K. (eds.), *Encycl. Snow, Ice and Glaciers*, Springer, Berlin (2011).
29. Zhu, M. et al. Mass balance of Muji Glacier, northeastern Pamir, and its controlling climate factors. *J. Hydrol.* **590**, 125447 (2020).
30. Zhou, Y., Li, Z., Li, J., Zhao, R. & Ding, X. Geodetic glacier mass balance (1975–1999) in the central Pamir using the SRTM DEM and KH-9 imagery. *J. Glaciol.* **65**, 309–320 (2019).
31. Chen, Y., Li, W., Deng, H., Fang, G., & Li, Z. Changes in Central Asia's water tower: past, present and future. *Scient. Rep.* **6**, 35458 (2016).
32. Biemans, H. et al. Importance of snow and glacier meltwater for agriculture on the Indo-Gangetic Plain. *Nature Sustain.* **2**, 594–601 (2019).
33. Akhundzadah, N.A., Soltani, S. & Aich, V. Impacts of climate change on the water resources of the Kunduz River, Afghanistan. *Climate* **8**,<bvertical-align:super;> </bvertical-align:super;>102 (2020).
34. Sidle, R.C. Strategies for smarter catchment hydrology models: incorporating scaling and better process representation. *Geosci. Lett.* **8**, 24 (2021).
35. Fan, Y., Chen, Y., Li, X., Li, W. & Li, Q. Characteristics of water isotopes and ice-snowmelt quantification in the Tizinafu River, north Kulun Mountains, Central Asia. *Quatern. Inter.* **380–381**, 116–122 (2015).
36. Gorbunov, A.P. Permafrost investigations in high-mountain regions. *Arct. Alpine Res.* **10**, 283–294 (1978).
37. Obu, J. et al. Northern Hemisphere permafrost map based on TTOP modelling for 2000–2016 at 1 $km^2$ scale. *Earth-Sci. Rev.* **193**, 299–316 (2019).
38. Osterkamp, T.E. & Burn, C.R. Permafrost. In: *Encyclopedia of Atmos. Sci.* (Holton, J.R. et al., eds.) 1st ed., 1717–1729, Elsevier Science, Amsterdam (2003).
39. Kim, H.-J., Sidle, R.C., Moore, R.D. & Hudson, R. Throughflow variability during snowmelt in a forested mountain catchment, coastal British Columbia, Canada. *Hydrol. Process.* **18**, 1219–1236 (2004).
40. Kraaijenbrink, P.D.A., Bierkens, M.F.P., Lutz, A.F. & Immerzeel, W.W. Impact of a global temperature rise of 1.5 degrees Celsius on Asia's glaciers. *Nature* **549**, 257–260 (2017).
41. Kaspari, S., Painter, T.H., Gysel, M., Skiles, S.M. & Schwikiowski, M. Seasonal and elevational variations of black carbon and dust in snow and ice in the Solu-Khumbu, Nepal and estimated radiative forcings. *Atmos. Chem. Physics* **14**, 8089–8103 (2014).
42. Marzeion, B. et al. Partitioning the uncertainty of ensemble projections of global glacier mass change. *Earth's Future* **8**, e2019EF001470 (2020).
43. Rounce, D.R., Hock, R. & Shean, D.E. Glacier mass change in High Mountain Asia through 2100 using the open-source Python Glacier Evolution Model (PyGEM). *Front. Earth Sci.* **7**, 331 (2020).

44. Wang, Q., Yi, S. & Sun, W. Precipitation-driven glacier changes in the Pamir and Hindu Kush mountains. *Geophys. Res. Lett.* **44**, 2817–2824 (2017).
45. de Kok, R.J., Kraaijenbrink, P.D.A., Tuinenburg, O.A., Bonekamp, P.N.J. & Immerzeel, W.W. Snowfall increase counters glacial demise in Kunlun and Karakoram. *The Cryosphere Discuss.*, 1–23 (2019).
46. Gardelle, J., Berthier, E., Arnaud, Y. & Kääb, A. Region-wide glacier mass balances over the Pamir-Karakoram-Himalaya during 1999–2011. *The Cryosphere* **7**, 1263–1286 (2013).
47. Knoche, M., Merz, R., Lindner, M. & Weise, S.M. Bridging glaciological and hydrological trends in the Pamir Mountains, Central Asia. Water **9**, 422 (2017).
48. Hall, D.K., Riggs, G.A. & Salomonson, V.V. *MODIS/terra snow cover daily L3 global 500m grid, version 6*. Boulder, CO: NASA National Snow and Ice Data Center Distributed Active Archive Center (2016).
49. Luo, D.L., Jin, H.J., Marchenko, S. & Romanovsky, V. Distribution and changes of active layer thickness (ALT) and soil temperature (TTOP) in the source area of the Yellow River using the GIPL model. *Science China Earth Sci.* **57**, 1834–1845 (2014).
50. Beven, K. Infiltration into a class of vertically non-uniform soils. *Hydrol. Sci. J.* **29**, 425–434 (1984).
51. Boike, J., Roth, K. & Overduin, P.P. Thermal and hydrologic dynamics of the active layer at a continuous permafrost site (Taymyr Peninsula, Siberia). *Water Resour. Res.* **34**, 355–363 (1998).
52. Sidle, R.C., Kim, K., Tsuboyama, Y. & Hosoda, I. Development and application of a simple hydrogeomorphic model for headwater catchments. *Water Resour. Res.* **47**, W00H13, (2011).
53. Randolph Glacier Inventory, *Randolph Glacier Inventory 6.0*. https://doi.org/10.7265/N5-RGI-60 (2017).

# Figures

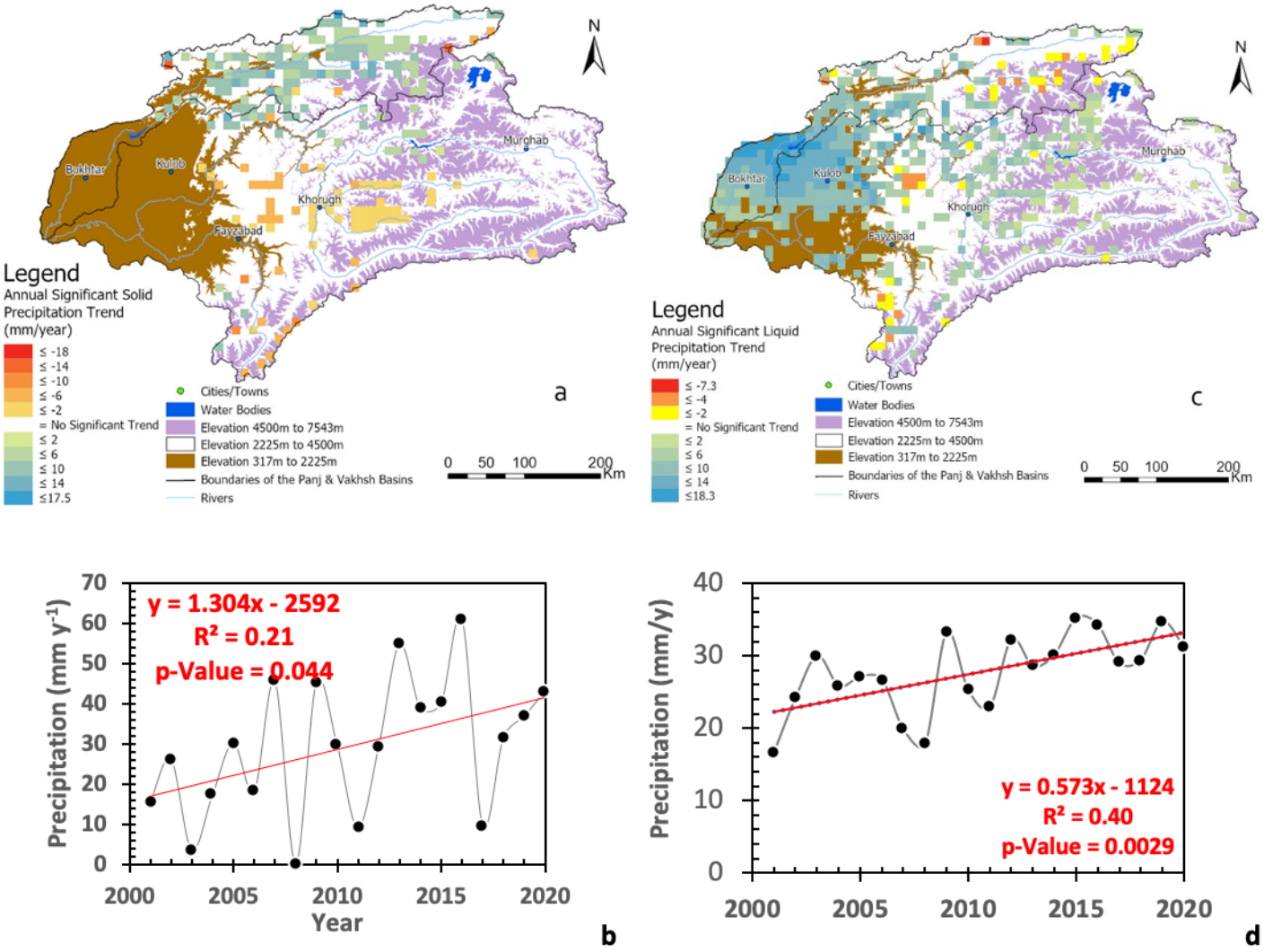


## Figure 1

(a) Changes in distributed snow water from 2001 to 2020 across three elevation bands (<2225 m; 2225-4500 m; and >4500 m) in the Vakhsh and Panj basins based on remotely sensed data. Color highlighted pixels (≈ 10 x 10 km) on the map indicate areas where significant (95% confidence level) changes have occurred. (b) An example of the increasing snow water trend in areas below 2225 m elevation (23 April to 20 May). (c) Changes in distributed rainfall from 2001 to 2020 across the three elevation bands. (d) Annual rainfall trends in low-elevation areas (317-2225 m).

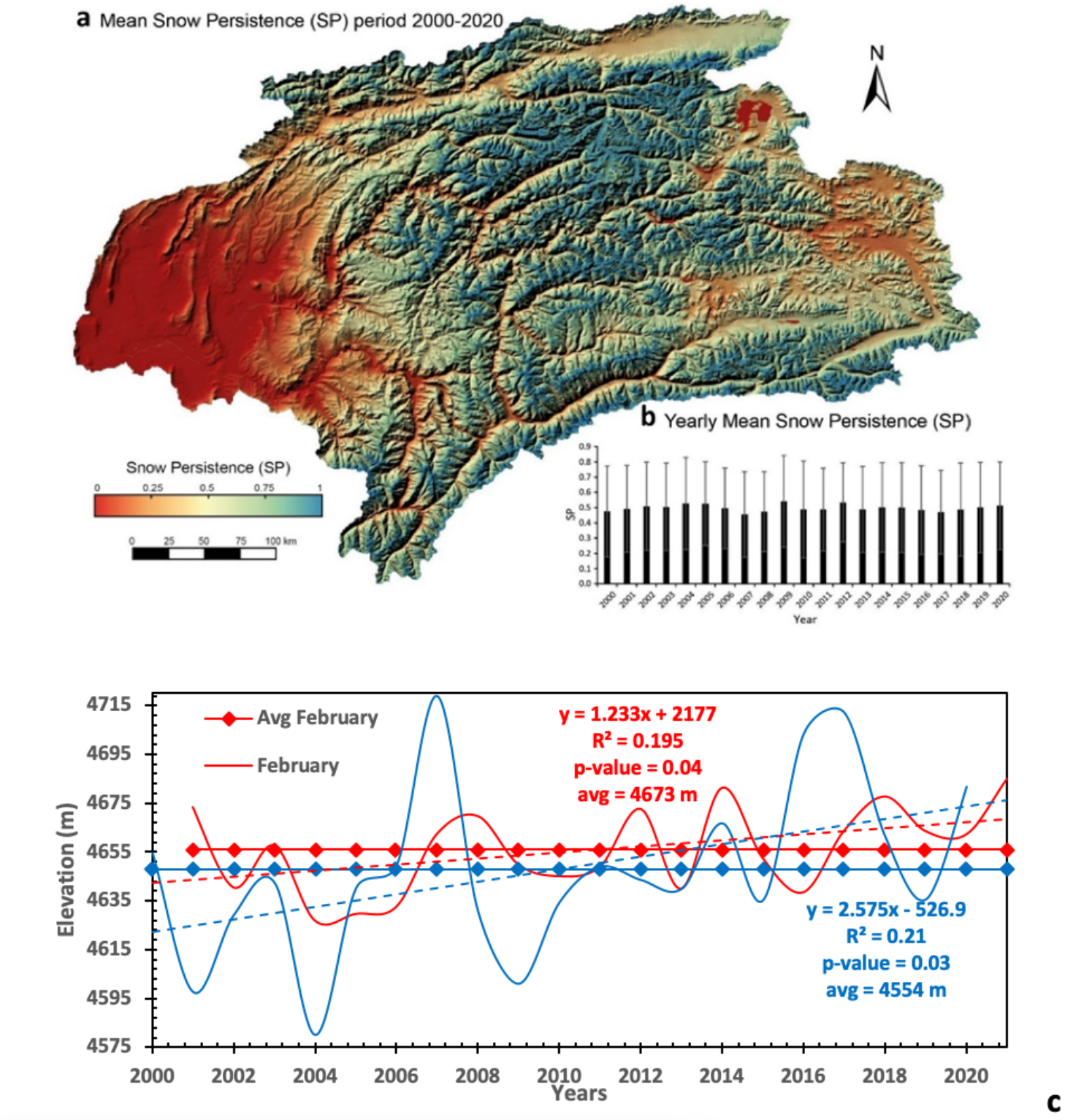


## Figure 2

(a) Mean snow persistence (SP) from 2000 to 2020 throughout the Vakhsh and Panj basins; (b) Annual mean snow persistence values from 2000 to 2020; temporal trend was not significant; (c) Snowline elevations in February and November in the high elevation range (> 4500 m) of Upper Amu Panj basin from 2000 to 2021 using MOD10A2.006 products. Significant trends are shown in dashed regression lines.

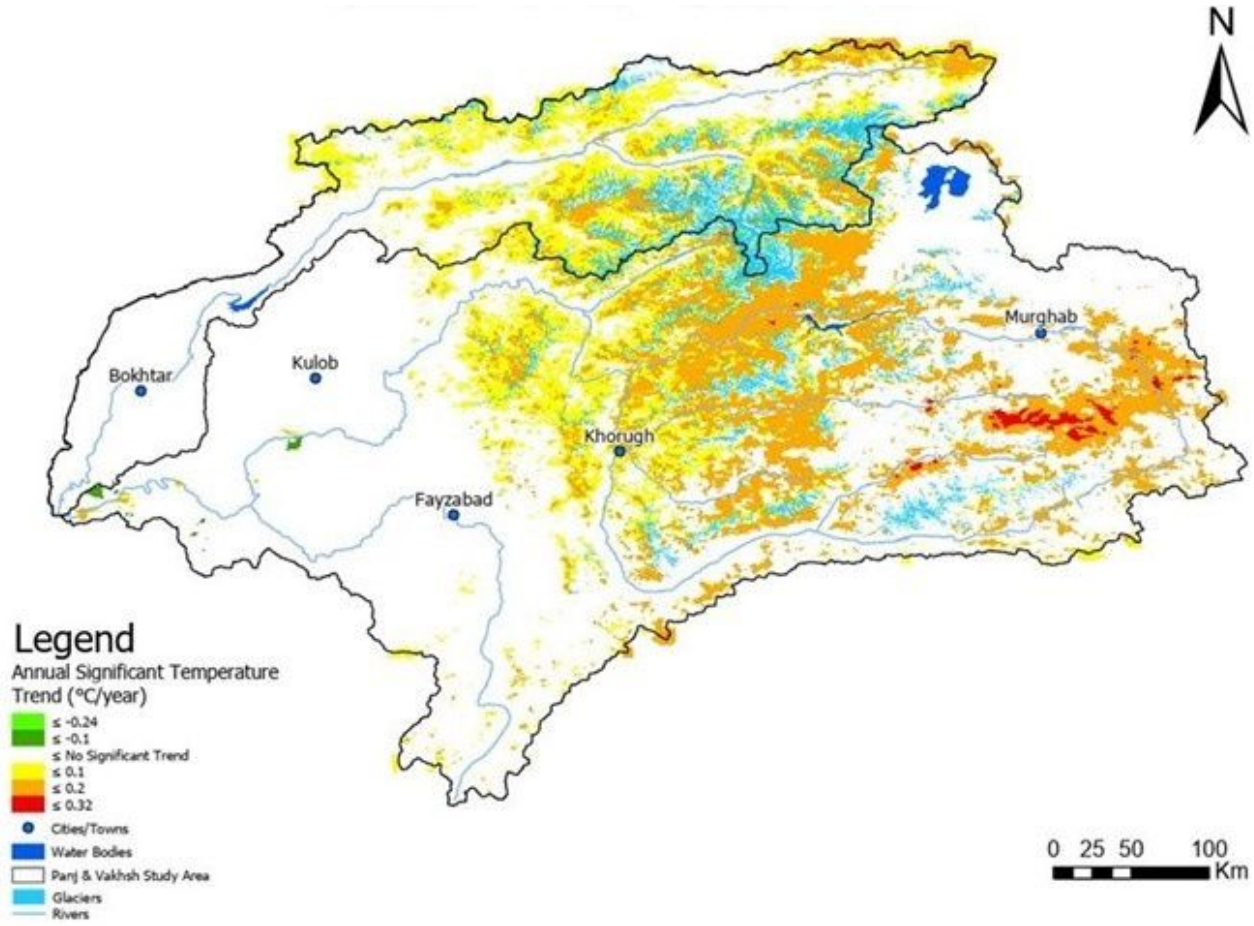


## Figure 3

MODIS-derived annual temperature changes across the Vakhsh and Panj basins from 2001 to 2020. Color highlighted pixels (≈ 10 x 10 km) indicate areas where significant (95% confidence level) changes have occurred. Glaciated areas appear in light blue color.

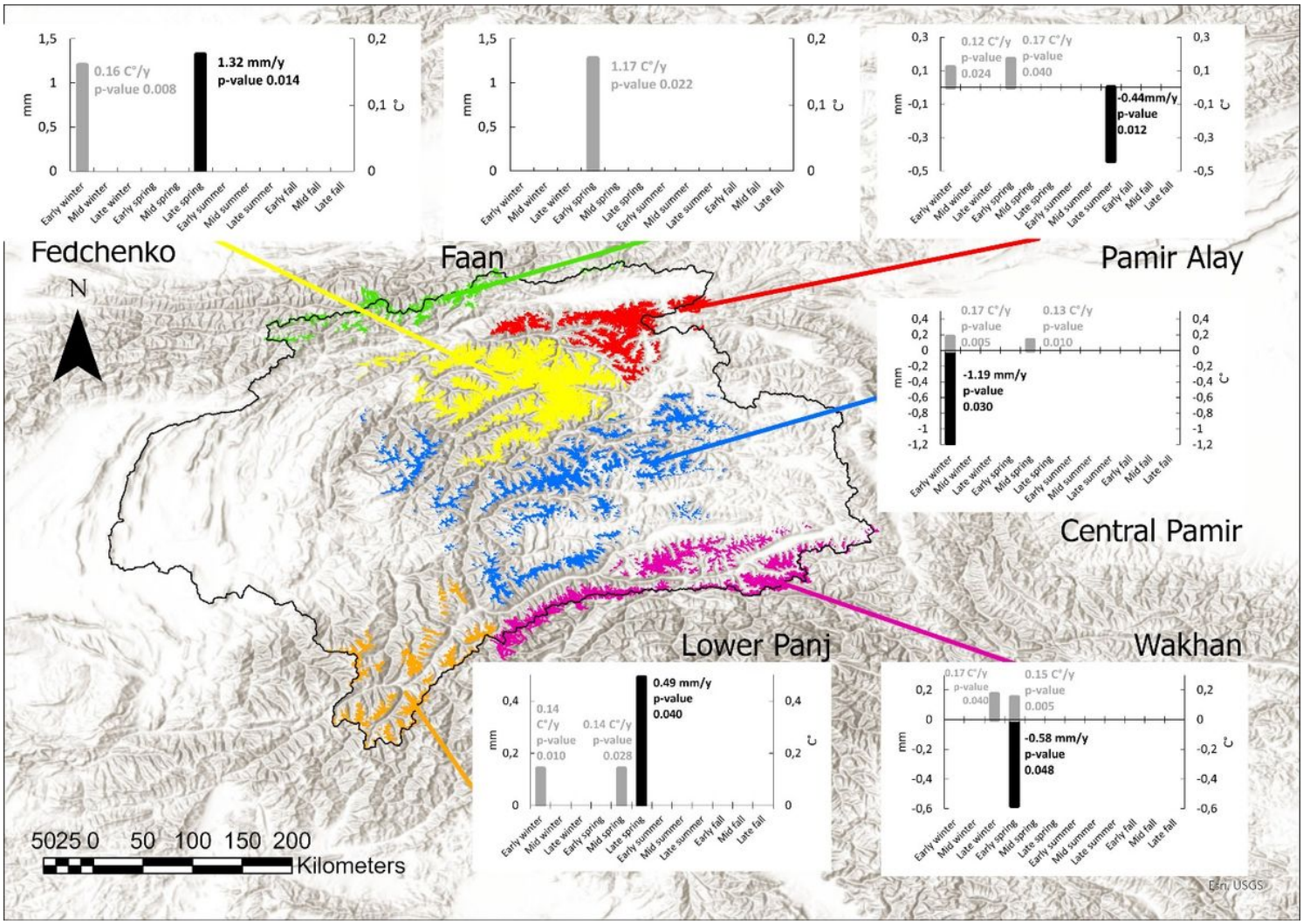


## Figure 4

Various glacier sectors in the Vakhsh-Panj basin derived from the Randolph Glacier Inventory (53): green, Fann Range; red, Pamir-Alay; yellow, Fedchenko glacier area; blue, Central Pamir; pink, Wakhan corridor; and orange, lower Panj basin. Graphs indicate when significant changes in temperature and solid precipitation occurred (expressed on an annual basis) within these glaciated areas.

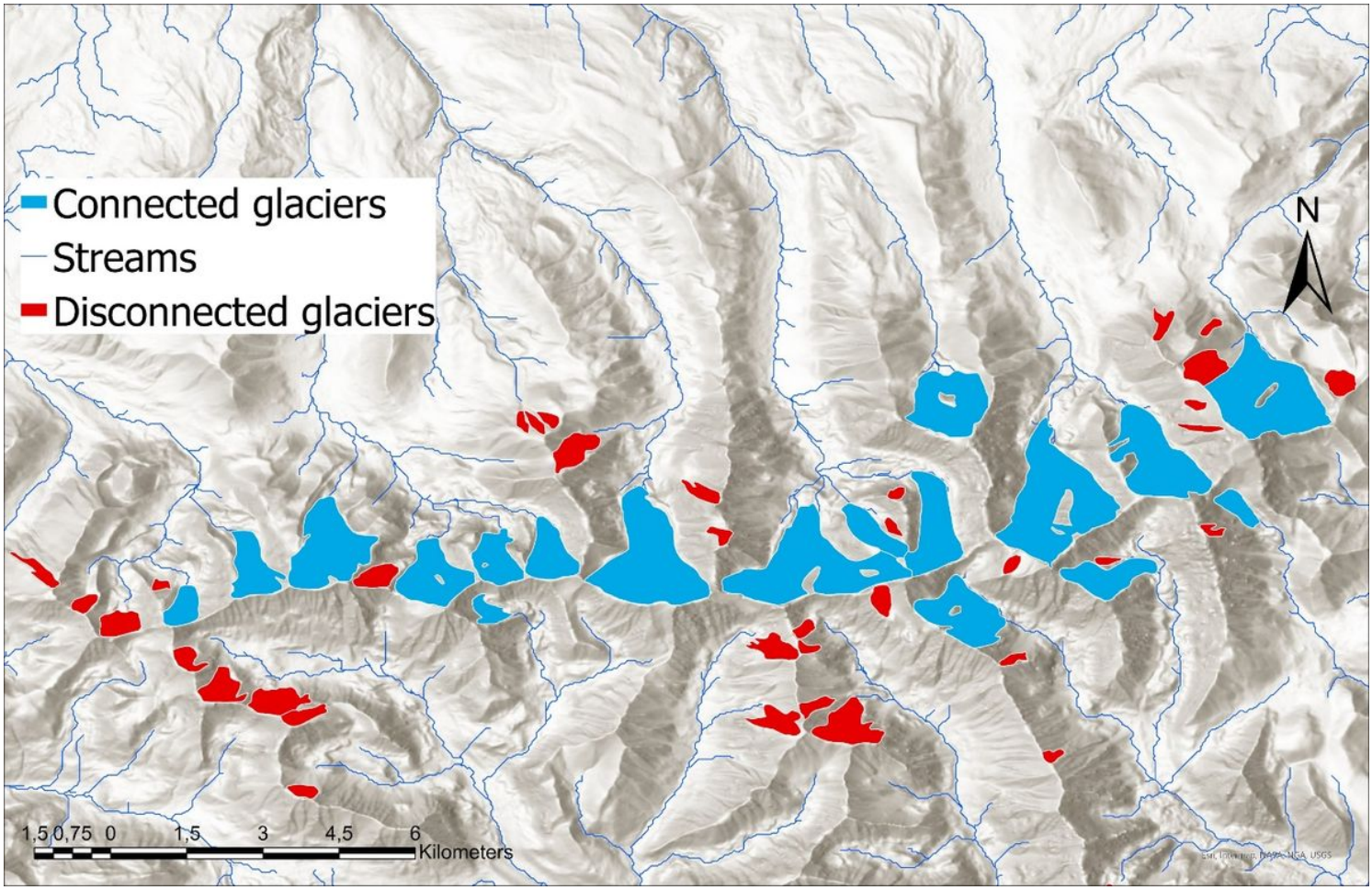


**Figure 5**

An example of the connectivity of glaciers to stream networks in eastern Pamir.

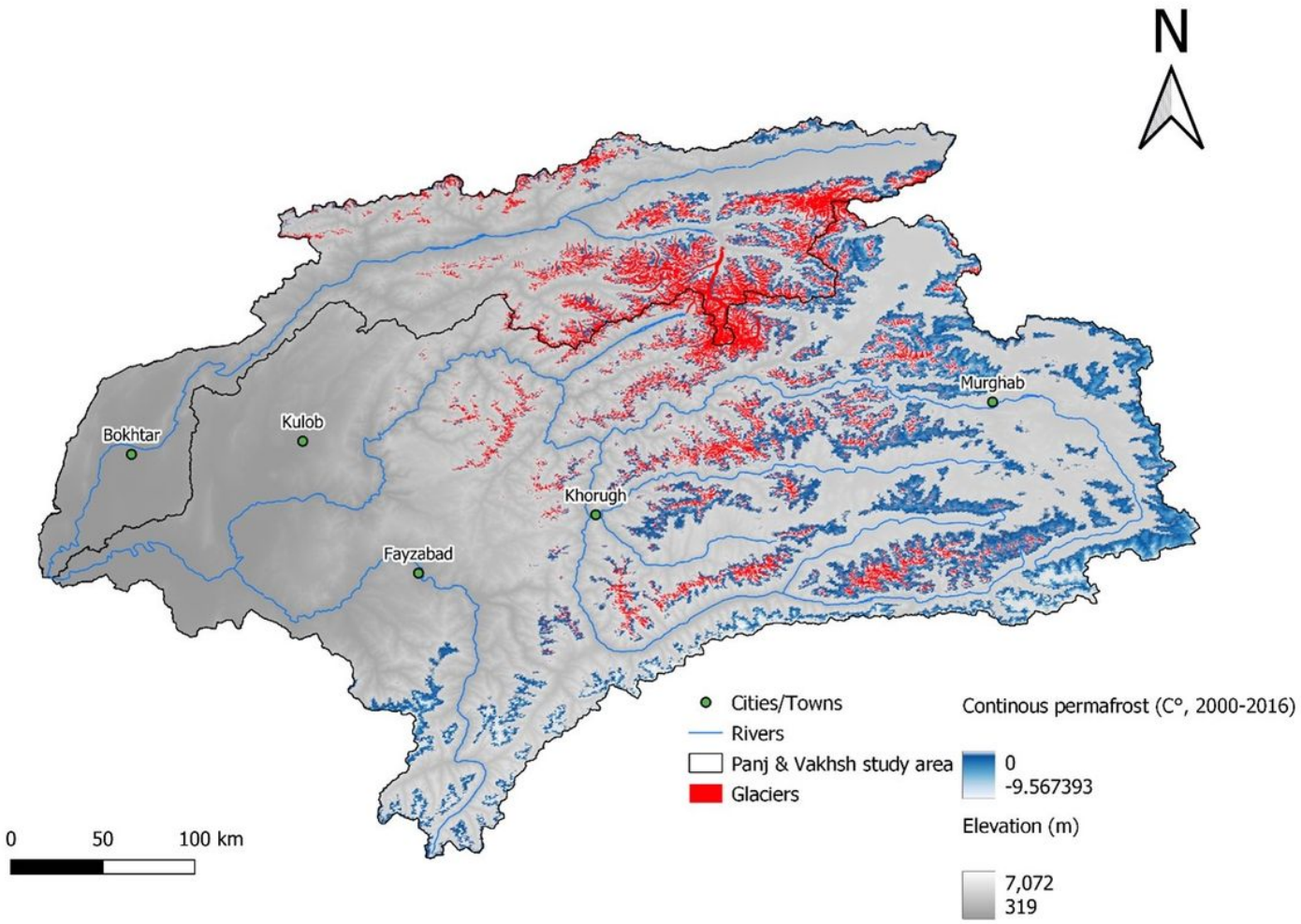


## Figure 6

Permafrost distribution in the Panj and Vakhsh basins based on the TTOP model (37).